

Linköping University Post Print

Interaction of $\cdot(\text{CH}_2\text{OH})$ with silver cation in Ag-A/ CH_3OH zeolite: A DFT study

Marek Danilczuk, Dariusz Pogocki and Anders Lund

N.B.: When citing this work, cite the original article.

Original Publication:

Marek Danilczuk, Dariusz Pogocki and Anders Lund, Interaction of $\cdot(\text{CH}_2\text{OH})$ with silver cation in Ag-A/ CH_3OH zeolite: A DFT study, 2009, CHEMICAL PHYSICS LETTERS, (469), 1-3, 153-156.

<http://dx.doi.org/10.1016/j.cplett.2008.12.060>

Copyright: Elsevier Science B.V., Amsterdam.

<http://www.elsevier.com/>

Postprint available at: Linköping University Electronic Press

<http://urn.kb.se/resolve?urn=urn:nbn:se:liu:diva-16742>

Interaction of $\cdot\text{CH}_2\text{OH}$ with silver cation in Ag-A/ CH_3OH zeolite: A DFT study

Marek Danilczuk^{1,*}, Dariusz Pogocki^{2,1}, Anders Lund³

¹ Institute of Nuclear Chemistry and Technology, Dorodna 16, 03-195 Warsaw, Poland

² Rzeszów University of Technology, Faculty of Chemistry, Powstańców Warszawy Ave. 35-959
Rzeszów, Poland

³ Department of Physics, Chemistry and Biology, IFM, Linköping University, S-581 83
Linköping, Sweden

Keywords: DFT, hydroxymethyl radical, zeolite A

*Corresponding author: Marek Danilczuk, Institute of Nuclear Chemistry and Technology

Dorodna 16, 03-195 Warsaw, Poland, Fax: +48-22-8111532, Tel: +48-22-8112347,

e-mail: mdan@orange.ichtj.waw.pl or danicma@udmercy.edu

Abstract

Density functional theory (DFT) has been applied to model the structure of $(\text{Ag}\cdot\text{CH}_2\text{OH}/\text{A})^+$ complexes previously experimentally characterized by electron paramagnetic resonance (EPR) in zeolite matrices. The magnetic parameters of $(\text{Ag}\cdot\text{CH}_2\text{OH}/\text{A})^+$ were found to depend on the local structure of the zeolite represented by clusters referred to as 3T and 6T, and also on the applied computational method. A spin distribution analysis confirms the one-electron silver-carbon bonding, showing delocalization of an unpaired electron density distributed between the silver and carbon atoms along the one-electron silver-carbon bond. The results are of relevance for a deeper understanding of the electronic and catalytic properties of zeolites containing silver atoms and clusters.

Introduction

Zeolites exchanged with different metal ions have drawn a lot of attention because of their chemical and electronic properties, especially for their catalytic activity in many important chemical processes. In the past few years, it has been clearly established that exchangeable cations, which compensate a negative charge of silica-alumina framework, play a crucial role in the adsorption and catalysis [1]. The electronic and chemical properties of transition metal ions and clusters formed in various inert gas matrices as well as in zeolites have been widely studied by numerous experimental techniques [2-5].

Due to variety of pore size and very high dispersion of metal atoms or ions the catalytic activity of synthetic zeolites as well as product formation selectivity can be controlled within the wide scope [6,7]. Differences in preparation and treatment procedures of zeolites may also have an effect on chemical states and dispersions of the cations, which will lead to marked differences in the catalytic properties. Zeolites containing transition metal ions exhibit unique ability to stabilize cationic metal clusters. Highly dispersed atoms or metal clusters formed by sublimation or irradiation of metal cations are much more reactive compared to the bulk. They can form complexes with many organic molecules – including radicals or ions. Such processes are based on specific interactions between the adsorbates and exchangeable cations [8-15].

Study of the interaction between transition-metal atoms, cations or clusters and small organic molecules has attracted much attention during the last few decades. Atoms or small metal clusters trapped in various inert gas matrices they can form complexes with organic molecules usually unstable in normal conditions. The interactions of silver, copper or nickel with organic

molecules and radicals stabilized in different matrices have been studied by various experimental techniques [16-20].

The formation of one-electron silver-carbon bonds between organic radicals and Ag^+ in frozen alcoholic solutions was postulated earlier [21,22]. Shields observed formation of silver-radical adduct in irradiated solution of silver salts in methanol and assigned the doublet EPR spectrum to Ag^+-OCH_3 [23]. An Analogous doublet with $A_{\text{iso}}(\text{Ag}) = 12.8 \text{ mT}$ was observed by Janes *et al.* with $A_{\text{iso}}(\text{Ag}) = 12.8 \text{ mT}$ in methanol solution of silver perchlorate γ -irradiated at 77 K and was assigned to $\text{Ag}\cdot\text{CH}_2\text{OH}^+$ adduct [24]. Similar EPR signals with $A_{\text{iso}}(\text{Ag}) = 13.0 \text{ mT}$ have been observed in γ -irradiated frozen solution of methanol and in glassy ethanol [25]. It has been suggested that the organosilver radicals are formed by reaction between Ag^+ cations and $\cdot\text{CH}_2\text{OH}$ and $\text{CH}_3\cdot\text{CHOH}$.

The same type of $\text{Ag}\cdot\text{CH}_2\text{OH}^+$ species formed during radiation processes has been detected in different types of zeolites. In γ -irradiated AgNa/A zeolite with adsorbed methanol and high content of Ag^+ a spectrum of $\text{Ag}\cdot\text{CH}_2\text{OH}^+$ with rather low silver hyperfine splitting, $A_{\text{iso}}(\text{Ag}) = 10.4 \text{ mT}$ appears directly after irradiation at 77 K. For low silver loading $\text{Ag}\cdot\text{CH}_2\text{OH}^+$ forms above 140 K due to higher separation of the reactants [26,27]. Further EPR study of organosilver radicals has shown that hyperfine splitting constants of $\text{Ag}\cdot\text{CH}_2\text{OH}^+$ doublets, stabilized in different molecular sieves, vary depending on the zeolite from 10.4 mT in zeolite A to 18 mT in SAPO-11 [28]. The results gathered so far show that the $\text{Ag}\cdot\text{CH}_2\text{OH}^+$ radical could be stable due to the formation of an one-electron bond between Ag and C atoms. However, the structure of $\text{Ag}\cdot\text{CH}_2\text{OH}^+$ radical is still an open question.

Application of quantum chemistry methods can here provide important information on the character of the adsorbate-zeolite systems. Recent development in computational chemistry has

allowed predictions of electronic and magnetic properties with a satisfactory accuracy but still the calculation of hyperfine coupling constants are usually limited to isolated (gas phase) organic radicals. There are, however, some literature data taking into account interaction of radicals with the surrounding [19,29,30]. However, due to the complexity of adsorbate-zeolite systems, the application of very sophisticated *ab initio* or density functional theory (DFT) methods for the calculations of magnetic parameters require quite substantial computational effort.

In this study we demonstrate that DFT calculations of hyperfine structure constants (hfsc) for the $\text{Ag}\cdot\text{CH}_2\text{OH}^+$ complex stabilized in Ag/A zeolite can lead to the determination of the geometry and the electronic structure of $\text{Ag}\cdot\text{CH}_2\text{OH}^+$ cation radical. Our attention in the geometry and electronic structure of the $\text{Ag}\cdot\text{CH}_2\text{OH}^+$ cation radical is fundamental for a deeper understanding of the hyperfine structure constants (hfsc's) induced by the complex formation with Ag^+ , and for elucidating the mechanism of the formation of organosilver radicals in zeolitic matrixes.

Methods

Alumina and silica tetrahedra in zeolite A are bonded together to form truncated octahedra called β -cages or sodalite units with a diameter of 1.14 nm which constitutes the channel structure of zeolite A (Fig. 1). The entrance of organic adsorbates to a sodalite unit from an α -cage is only possible through a six-membered ring, called a hexagonal window. Its diameter of 0.22 nm is too small to let organic adsorbate get into sodalite. The framework of zeolite A consists of one α and eight β cages per unit cell. The cation capacity of zeolite A is 12 cations per unit cell.

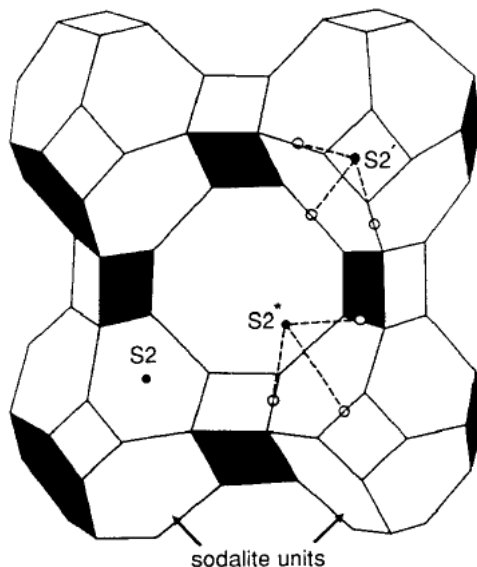


Figure 1. Schematic diagram of the zeolite A structure. Each vertex represents an Al or Si atom and the lines represent O bridges.

In our calculations the local structure A zeolite was represented by 3T and 6T clusters. This approach has been proven to give reliable results for the $\bullet\text{CH}_3\cdots\text{Na}^+\text{-A}$ system [30]. In order to represent active Lewis sites each cluster contains one AlO_4^- group. The negative charge introduced by the AlO_4^- group is balanced by the Ag^+ cation. The model clusters used were larger than usually applied ones, since H terminal atoms were replaced by -OH groups. The H

atoms were located at a distance of 1 Å from the corresponding oxygen atom, and with the O-H bond oriented along the bond direction to the next Si or Al atom in the zeolite framework. The location of Si and O atoms were fixed in their crystallographic positions [2,31-34], see Figure 2. Importantly, due to applied constrains harmonic frequencies calculations cannot be performed to confirm that both models correspond to total energy minima.

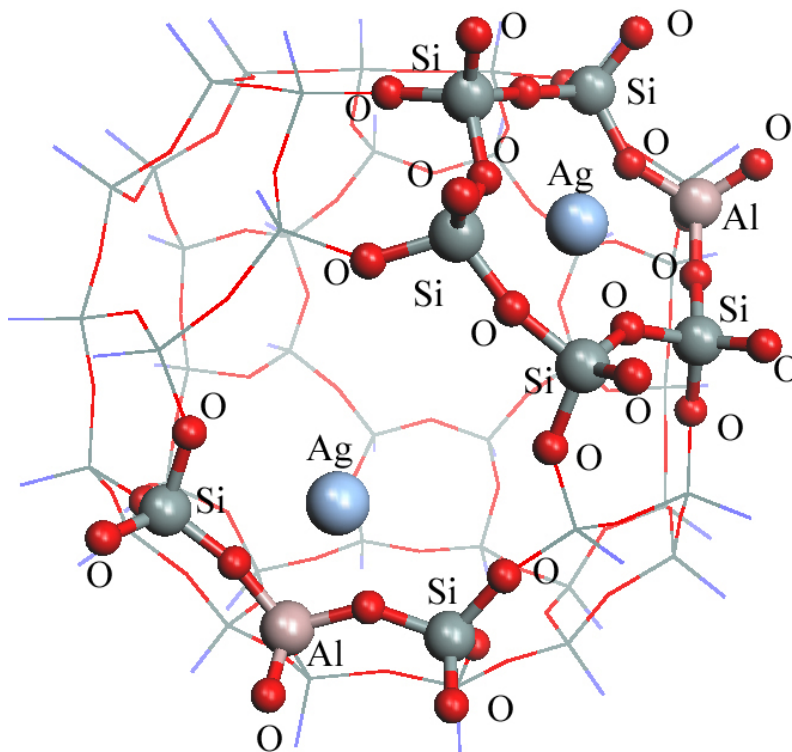


Figure 2. Representation of Ag(I)/A 3T and 6T cluster clusters.

First principles density functional calculations were performed using B3LYP functional [35,36] implemented in the Gaussian 03 program [37] and LANL2DZ basis set. The core electrons of the Ag atom were represented by LANL2DZ effective core potential (ECP) from the 28-electrons of the Ag core, and its valence electrons were described by LANL2DZ basis supplemented with one f-function [38].

The magnetic parameters were calculated with the ORCA package [39]. The g-tensor were calculated according to the coupled-perturbed Kohn-Sham approximation [40] and A-tensors were calculated according to the procedure of van Lenthe in the ZORA (zero-order regular approximation) formalism [41] implemented in Orca package. Calculations of the magnetic properties of Ag atoms were performed with a combination of B3LYP or BP86 functionals and uncontracted DGDZVP basis sets [42].

Results and discussion

Structure of Ag/A

It can be expected that in fully exchanged dehydrated zeolite Ag₁₂/A Ag⁺ cations are located at sites like those found for other cations in the structures of dehydrated zeolite X/A (X= Na⁺, K⁺, Rb⁺) [2,3,43]. In the fully exchanged form each of the eight Ag⁺ is located in the center of a hexagonal window, three are associated with 8-membered rings and one Ag⁰ would be located near the 4-membered ring [44]. However, in zeolite with lower Ag⁺ loading silver cations prefer position nearly at the center of the hexagonal window [2] (see Figure 1).

The CH₃OH molecules are too large to get access into the β-cages through hexagonal windows of diameter *ca.* 0.22 nm. Therefore, it seems reasonable to assume that after adsorption, methanol molecules are present only in the α-cages and hydroxymethyl radicals are also formed there. So, it is reasonable to assume that only Ag⁺ cation located in the hexagonal windows or in the vicinity of octagonal windows can form (Ag•CH₂OH)⁺ complex.

In Ag-exchanged zeolite, the silver cation does not form bonds with a particular atom, but is coordinated by oxygen atoms of the zeolite framework. The optimized Ag/A (3T) cluster

representing a fragment of an octagonal window and the Ag/A (6T) cluster corresponding to a hexagonal window are shown in Figure 3. The structures reported in Figure 3 correspond to local energy minima. In the 3T cluster of Ag/A zeolite, the Ag^+ doesn't bind to any particular atom, but rather is symmetrically bonded to two oxygen atoms of an AlO_4^- unit. In the 3T cluster the Ag^+ cation is located 2.288 and 2.417 Å from the nearest oxygen atoms as can be deduced from Figure 3.

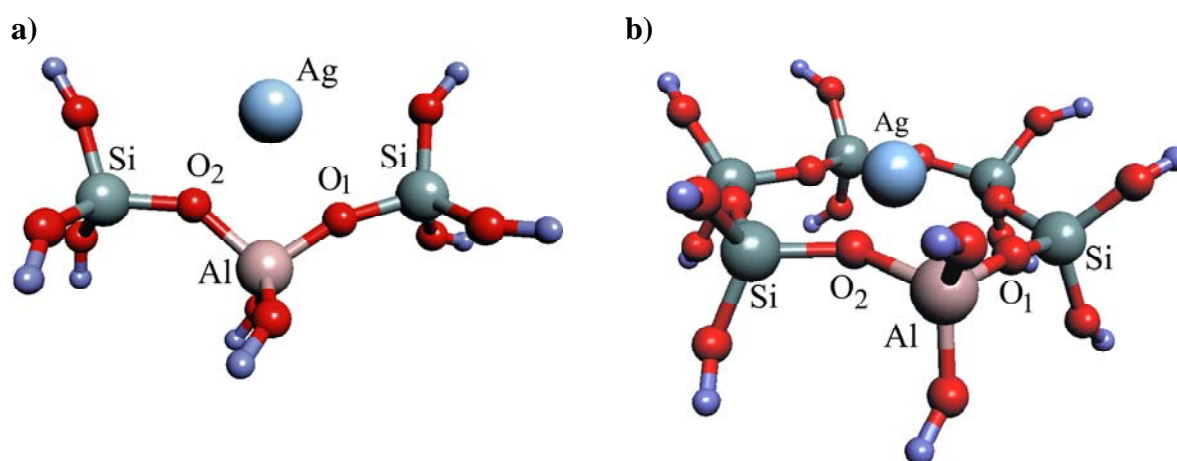


Figure 3. Optimized structures of Ag^+ on zeolite A; (a) 3T and (b) 6T cluster

In the 6T cluster Ag^+ occupies a position near the window center. Presence of Al atom in the 6-membered ring does not affect much the position of the Ag^+ cation. The distances to the nearest oxygen atoms of the zeolite framework are 2.23, 2.34 and 2.48 Å. The Ag^+ cation is a little bit shifted from the center of hexagonal window to the oxygen atoms of the AlO_4^- unit.

Experimental data indicate that the Ag^+ cation occupies a position in the center of the hexagonal window of zeolite A and is trigonally coordinated by nearest oxygen atoms of zeolite framework with distances of 2.23 and 2.25 Å. All calculated structural parameters are in line with those obtained by X-ray or neutron diffraction in fully or partially exchanged zeolite Ag/A

[2,43]. Table 1 summarizes the most important structural parameters, representative for the investigated models of Ag/A zeolite. These preliminary steps allowed validating the size of the clusters examined in this study.

Table 1. Selected structural parameters for Ag/A(3T) and Ag/A(6T) clusters (bond lengths are in Å and bond angles are in °)

Parameters	Ag/A	
	3T	6T
Ag-O1	2.29	2.23
Ag-O2	2.42	2.34
Ag-O3	-	2.48
Al-O1	1.67	1.66
Al-O2	1.70	1.65
O1-Al-O2	105.15	104.51

Structure of (Ag•CH₂OH/A)⁺

The optimized geometries of hydroxymethyl radical (•CH₂OH) adsorption complexes on Ag-A zeolite are shown in Figure 4. The •CH₂OH radical interacts with the Ag⁺ cation forming an adsorption complex stabilized *via* an one-electron bond [45]. The distance between Ag⁺ and the •CH₂OH radical varies from 2.358 to 2.349 Å for 3T and 6T clusters, respectively, indicating relatively strong interaction between the radical and the Ag⁺ cation. The distances between the Ag⁺ cation and the nearest oxygen atoms of the zeolite framework are slightly lengthened in the presence of •CH₂OH compared to the bare clusters, in the absence of •CH₂OH radical for both of the applied models of Ag/A zeolites. This can indicate that the interaction of the Ag⁺ cation with the zeolite framework is weaker after formation of the (Ag•CH₂OH)⁺ complex. Such a small difference in the distances between Ag⁺ and •CH₂OH radical for both applied models may indicate that the size of the used structure mimicking the zeolite framework does not much affect

the geometry of the $(\text{Ag}\cdot\text{CH}_2\text{OH})^+$ complex. Selected structural parameters of the adduct complexes are listed in Table 2.

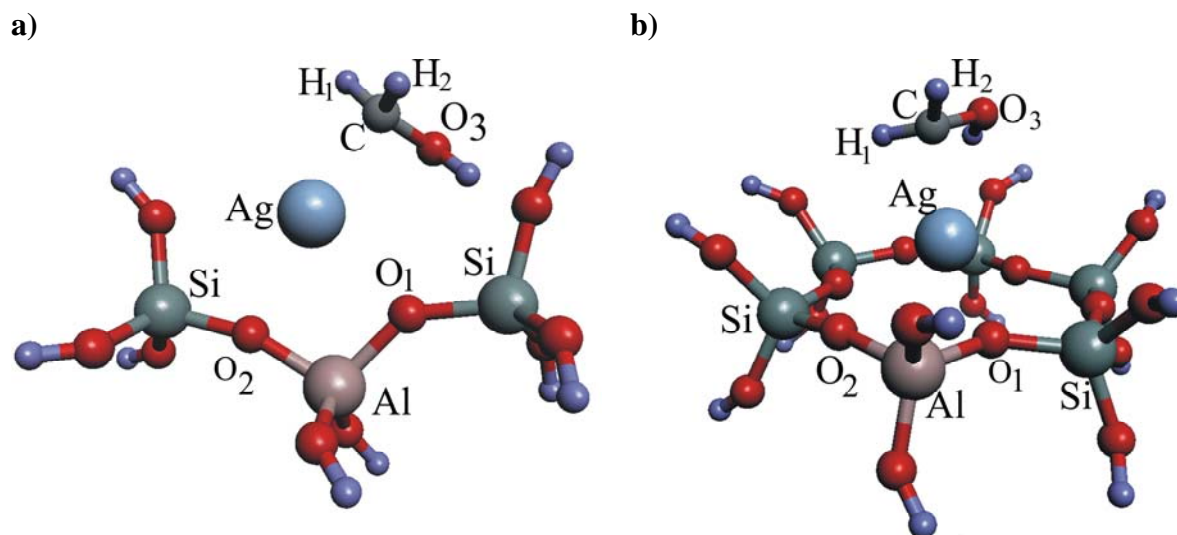


Figure 4. Optimized structures of $(\text{Ag}\cdot\text{CH}_2\text{OH})^+$ complex on zeolite A; (a) 3T and (b) 6T cluster

Table 2. Selected structural parameters for $(\text{Ag}\cdot\text{CH}_2\text{OH})^+/\text{A}(3\text{T})$ and $(\text{Ag}\cdot\text{CH}_2\text{OH})^+/\text{A}(6\text{T})$ complexes (bond lengths are in Å and bond angles are in °)

Parameters	$(\text{Ag}\cdot\text{CH}_2\text{OH}/\text{A})^+$	
	3T	6T
Ag-O ₁	2.36	2.29
Ag-O ₂	2.48	2.59
Ag-O ₃	-	2.86
Al-O ₁	17.1	1.67
Al-O ₂	17.3	1.65
Ag-C	2.26	2.36
O1-Al-O2	104.56	104.47
O1-Ag-C	105.34	158.51
Ag-C-O3	101.78	108.22
H1-C-H2	117.56	118.79

Magnetic parameters of $(\text{Ag}\cdot\text{CH}_2\text{OH}/\text{A})^+$

Based on the experimental values of the hyperfine coupling constants it was estimated that 46 % of the spin density is localized on C and H and 29% on the Ag atom. By comparison with

the spin density on C and H atoms of the isolated $\bullet\text{CH}_2\text{OH}$ radical which is about 70 % it was concluded that the $\bullet\text{CH}_2\text{OH}$ radical in the Ag-A zeolite shares its unpaired electron with the Ag^+ cation and is able to form $(\text{Ag}\bullet\text{CH}_2\text{OH})^+$ silver hydroxymethyl radical [28].

The calculated magnetic parameters of the two investigated models of the $(\text{Ag}\bullet\text{CH}_2\text{OH})^+$ complex are listed in Table 3 for the ^{109}Ag isotope, present in 48.161 % natural abundance. The hyperfine coupling parameters for the ^{107}Ag isotope in 51.839 % abundance can be obtained by multiplication with the ratio 0.8690 between their magnetic moments. Since the experimentally observed EPR spectra had an isotropic appearance [26-28] we do not discuss anisotropic hyperfine coupling and g -tensor parameters obtained in the calculations. However, both isotropic and anisotropic values are presented in the table. The isotropic hyperfine couplings of the $(\text{Ag}\bullet\text{CH}_2\text{OH})^+$ complex calculated at the B3LYP/DGDZVP level are equal to $A_{\text{iso}}(3\text{T}) = 16.83$ mT for ^{109}Ag and $A_{\text{iso}}(6\text{T}) = 14.21$ mT for ^{107}Ag , in relatively good agreement with the experimental values obtained in various molecular sieves [26-28].

Table 3. Calculated magnetic parameters for $\text{Ag}\bullet\text{CH}_2\text{OH}^+$ complex obtained with B3LYP and BP86 functional and DGDZVP basis sets. (^{109}Ag hyperfine couplings constants are in mT. The hyperfine coupling constants for the ^{107}Ag isotope can be obtained by multiplication with the factor 0.8690).

exp	3T		6T	
	B3LYP	BP86	B3LYP	BP86
A_1	- 16.31	- 8.42	- 13.79	- 7.07
A_2	- 16.54	- 8.60	- 13.85	- 7.12
A_3	- 17.34	- 9.52	- 14.99	- 8.03
A_{iso} 11.32*	- 16.83	- 8.85	- 14.21	- 7.41
g_1	1.9983	2.0005	1.9987	2.0016
g_2	2.0038	2.0039	2.0022	2.0027
g_3	2.0165	2.0172	2.0110	2.0127
g_{iso} 2.003	2.0062	2.0072	2.0040	2.0057

* experimental hfc of $\text{Ag}\bullet\text{CH}_2\text{OH}^+$ complex observed in $\text{Ag}_1\text{Na}/\text{A}$ zeolite.²⁵

The $\bullet\text{CH}_2\text{OH}$ has a non planar structure and the radical electron is delocalized between the carbon and the oxygen atoms in a π_{CO}^* orbital.[46] An NBO (*Natural Bond Orbital*) analysis shows that in $(\text{Ag}\bullet\text{CH}_2\text{OH})^+$ complex *ca.* 21 % and 18 % spin density for 3T and 6T clusters, respectively, migrates to the 5s orbital of the silver. Lower spin density on Ag in the 6T model leads to a decreased calculated Ag hyperfine coupling constant, which can be attributed to the difference in coordination of Ag^+ by nearest oxygen atoms of the zeolite framework. The values of isotropic hyperfine constants provided by DFT calculations confirmed considerable difference between the two applied models.

As can be seen from Table 2 calculations with the BP86 functional produced significantly underestimated values of hfsc's for both applied models.

Generalized gradient approximation (GGA) functionals, such as the BP86 functional overestimate the covalency of the polar metal-ligand bonds. This leads to underestimating the spin density on the metal nucleus using the BP86 functional. The overestimated covalency leads also to a higher g-factor at the BP86 functional level [47].

Overestimated covalency is also visible in the higher g-factors produced with the BP86 functional, 2.0072 and 2.0057 for the 3T and 6T cluster, respectively, compared to the experimental value 2.003. The g-factors calculated with B3LYP are lower than obtained with the BP86 functional, 2.0062 and 2.0040 for the 3T and 6T models, respectively. The B3LYP functional leads to larger metal hfsc's and to g-factors that are closer to the experimental values.

Conclusions

The DFT calculations shows that calculated magnetic parameters of $(\text{Ag}\bullet\text{CH}_2\text{OH}/\text{A})^+$ depend on the local structure of zeolite represented by 3T and 6T clusters, and the applied computational

method. Both hfsc's and g -factor were satisfactory reproduced at the B3LYP/DGDZVP level for the 6T cluster. The spin distribution analysis shows that spin delocalization occurs along $\text{Ag}\cdot\text{CH}_2\text{OH}^+$.

Reference List

- [1] A. Chatterjee, F. Mizukami, *Chemical Physics Letters* 385 (2004) 20.
- [2] Y. Kim, K. Seff, *J. Phys. Chem.* 91 (1987) 671.
- [3] Y. Kim, K. Seff, *J. Phys. Chem.* 82 (1978) 1071.
- [4] P.H. Kasai, D. McLeod, *J. Am. Chem. Soc.* 100 (1968) 625.
- [5] P.H. Kasai, P.M. Jones, *J. Phys. Chem.* 90 (1986) 4239.
- [6] J. Michalik, J. Sadlo, M. Danilczuk, J. Perlinska, H. Yamada, *Stud. Surf. Sci. and Catal.* 142 (2003) 311.
- [7] J. Michalik, J. Sadlo, M. Danilczuk, *Sol. State. Phen.* 94 (2003) 197.
- [8] D. Biglino, H. Li, R. Erickson, A. Lund, H. Yahiro, M. Shiotani, *Phys. Chem. Chem. Phys.* 1 (1999) 2887.
- [9] P.H. Kasai, D. McLeod, T. Watanabe, *J. Am. Chem. Soc.* 99 (1977) 3521.
- [10] P.H. Kasai, P.M. Jones, *J. Am. Chem. Soc.* 107 (1985) 813.
- [11] P.H. Kasai, *J. Am. Chem. Soc.* 106 (1984) 3069.
- [12] P.H. Kasai, *J. Phys. Chem.* 94 (1990) 3539.
- [13] M. Shiotani, F. Yuasa, J. Sohma, *J. Phys. Chem.* 79 (1975) 2669.
- [14] H. Yahiro, K. Kurohagi, G. Okada, Y. Itagaki, M. Shiotani, A. Lund, *Phys. Chem. Chem. Phys.* 4 (2002) 4255.
- [15] K. Ghandi, F.E. Zahariev, Y.A. Wang, *J. Phys. Chem. A* 109 (2005) 7242.
- [16] V. Doan, P.H. Kasai, *J. Phys. Chem. A* 101 (1997) 8115.
- [17] P.H. Kasai, D. McLeod, T. Watanabe, *J. Am. Chem. Soc.* 102 (1980) 179.
- [18] G.A. Ozin, W.J. Power, T.H. Upton, W.A. Goddard, *J. Am. Chem. Soc.* 100 (1978) 4750.

- [19] Z. Sojka, P. Pietrzyk, G. Martra, M. Kermarec, M. Che, *Catal. Today* 114 (2006) 154.
- [20] J.H.B. Chenier, J.A. Howard, B. Mile, *J. Am. Chem. Soc.* 107 (1985) 4190.
- [21] C.K. Alesbury, M.C.R. Symons, *J. Chem. Soc. Faraday Trans. I* 76 (1980) 244.
- [22] M.C.R. Symons, C.K. Alesbury, *J. Chem. Soc. Faraday Trans. I* 78 (1982) 3629.
- [23] L. Shields, *Trans. Faraday Soc.* 62 (1966) 1042.
- [24] R. Janes, A.D. Stevens, M.C.R. Symons, *J. Chem. Soc. , Faraday Trans.* 85 (1989) 3973.
- [25] M.C.R. Symons, R. Janes, A.D. Stevens, *Chem. Phys. Lett.* 160 (1989) 386.
- [26] A. van der Pol, J. Michalik, E. Reijerse, E. de Boer, *J. Phys. Chem.* 100 (1996) 3728.
- [27] T. Wasowicz, J. Mikosz, J. Sadlo, J. Michalik, *J. Chem. Soc. ,Perkin Trans. 2* 9 (1992) 1487.
- [28] J. Michalik, J. Sadlo, A. van der Pol, E. Reijerse, *Acta Chem. Scand.* 51 (1997) 330.
- [29] Z. Sojka, P. Pietrzyk, *Spectrochim. Acta A* 63 (2006) 788.
- [30] M. Danilczuk, D. Pogocki, A. Lund, J. Michalik, *J. Phys. Chem. B* 110 (2006) 24492.
- [31] N.H. Heo, W. Cruz-Patalinghug, K. Seff, *J. Phys. Chem.* 90 (1986) 3931.
- [32] N.H. Heo, S.H. Kim, W.T. Lim, K. Seff, *J. Phys. Chem. B* 108 (2004) 3168.
- [33] K. Seff, *Acc. Chem. Res.* 9 (1976) 121.
- [34] V. Subramanian, K. Seff, *J. Phys. Chem.* 81 (1977) 2249.
- [35] A.D. Becke, *J. Chem. Phys.* 98 (1993) 5648.
- [36] C.T. Lee, W.T. Yang, R.G. Parr, *Physical Review B* 37 (1988) 785.
- [37] M.J. Frisch, G.W. Trucks, H.B. Schlegel, G.E. Scuseria, M.A. Robb, J.R. Cheeseman, J.A. Montgomery Jr, T. Vreven, K.N. Kudin, J.C. Burant, J.M. Millam, S.S. Iyengar, J. Tomasi, V. Barone, B. Mennuchi, M. Cossi, G. Scalmani, N. Rega, G.A. Petersson, H. Nakatsuji, M. Hada, M. Ehara, K. Toyota, R. Fukuda, J. Hesagawa, M. Ishida, T. Nakajima, Y. Honda, O. Kitao, H. Nakai, M. Klene, X. Li, J.E. Knox, H.P. Hratchian, J.B. Cross, V. Bakken, C. Adamo, E. Jaramillo, R. Gomperts, R.E. Stratmann, O. Yazyev, A.J. Austin, R. Cammi, C. Pomelli, J.W. Ochterski, P.Y. Ayala, K. Morokuma, G.A. Voth, P. Salvador, J.J. Dannenberg, V.G. Zakrzewski, S. Dapprich, A.D. Daniels, M.C. Strain, O. Farkas, D.K. Malick, A.D. Rabuck, K. Raghavachari, J.B. Foresman, J.V. Ortiz, Q. Cui, A.G. Baboul, S. Clifford, J. Cioslowski, B.B. Stefanov, G. Liu, A. Liashenko, P. Piskorz, I. Komaromi, R.L. Martin, D.J. Fox, T. Keith, M.A. Al-Laham,

C.Y. Peng, A. Nanayakkara, M. Challacombe, P.M. Gill, W. Chen, M.W. Wong, C. Gonzalez, J.A. Pople, 2004)

- [38] P.J. Hay, W.R. Wadt, *J. Chem. Phys.* 82 (1985) 299.
- [39] F. Neese, 2007)
- [40] F. Neese, *J. Chem. Phys.* 115 (2001) 11080.
- [41] E. van Lenthe, J.G. Snijders, E.J. Baerends, *J. Chem. Phys.* 105 (1996) 6505.
- [42] N. Godbout, D.R. Salahub, J. Andzelm, E. Wimmer, *Can. J. Chem.* 70 (1992) 560.
- [43] Y. Kim, K. Seff, *J. Am. Chem. Soc.* 99 (1977) 7055.
- [44] Y. Kim, K. Seff, *J. Am. Chem. Soc.* 100 (1978) 6989.
- [45] J. Michalik, J. Sadlo, M. Danilczuk, J. Turek, *Res. Chem. Intermed.* 33 (2007) 793.
- [46] M.E. Jacox, D.E. Milligan, *Journal of Molecular Spectroscopy* 47 (1973) 148.
- [47] F. Neese, *J. Phys. Chem. A* 105 (2001) 4290.